Theoretical analysis of the mass balance equation through a flame at zero and non-zero Mach numbers

Michael Bauerheim, Franck Nicoud, Thierry Poinsot

Theoretical analysis of the mass balance equation through a flame at zero and non-zero Mach numbers

Michael Bauerheim [a,b,*], Franck Nicoud [c], Thierry Poinsot [d]

[a] CERFACS, CFD Team, 42 Av Coriolis, 31057 Toulouse, France
[b] Société Nationale d'Etude et de Construction de Moteurs d'Aviation, 77550 Reau, France
[c] Université Montpellier 2, I3M UMR CNRS 5149, France
[d] IMF Toulouse, INP de Toulouse and CNRS, 31400 Toulouse, France

ARTICLE INFO

Article history:
Received 20 February 2014
Received in revised form 25 June 2014
Accepted 25 June 2014
Available online 24 July 2014

Keywords:
Mass
Volume
Conservation
Mach number
Entropy
Singularities

ABSTRACT

This paper discusses a classical paradox in thermoacoustics when jump conditions are derived for acoustic waves propagating through a thin flat flame. It shows why volume conservation must be used for perturbations at zero Mach number (continuity of $v' = u'A$) while mass conservation is used at non-zero Mach numbers (continuity of $m' = \bar{\rho}_0 u'A + \bar{u}_0 \rho' A$). First, from the three-dimensional mass balance equation, a quasi one-dimensional mass balance equation is obtained for surface-averaged quantities. Then it is demonstrated that the acoustic and entropy disturbances are coupled and need to be solved together at the flame front because singularities in the entropy profile affect mass conservation. At non-zero Mach number, the entropy generated in the thin flame is convected by the mean flow: no singularity occurs and leads to the classical mass conservation at the interface. However, at zero Mach number, the flow is frozen and entropy spots are not convected downstream: they produce a singularity at the flame front due to the mean density gradient, which acts as an additional source term in the mass conservation equation. The proper integration of this source term at zero Mach number leads, not to the mass, but to the volume flow rate conservation of perturbations. A balance equation for the volume flow rate has been also derived. This equation couples the volume flow rate and the mean and fluctuating pressure. This latter equation degenerates naturally toward the volume flow rate conservation at the flame interface at zero Mach number because of the pressure continuity. This theoretical analysis has been compared to LEE (Linearized Euler Equation) simulations of stable flames and a good agreement is found for the entropy fluctuations shape and the conserved quantities.

1. Introduction

Acoustics remains a crucial topic in the development of modern gas turbines: acoustic waves can propagate in the whole combustion chamber, interacting with the compressor exit, the turbine stator inlet or the flames, leading to the production of direct [1–3] and indirect noise [4–8], vibrations and combustion instabilities [9–13].

Describing the acoustic modes, which can appear in combustion chambers and finding methods to control them has been the topic of multiple studies over the last decades [9,11,12,14–20]. The complexity and the cost of performing laboratory-scale experiments explain why progress in this field has been slow for a long time since. Recently, new well-instrumented acoustic experiments [7,14,21,22] have opened the path to investigate flame response to acoustics [23], direct and indirect noise [7] as well as combustion instabilities [10,14,15,21,22]. In addition, theoretical and numerical approaches have progressed in different directions: (1) three-dimensional high fidelity simulations of combustion chambers have been performed [24–27], (2) three-dimensional acoustic tools have been developed [28–31] and (3) analytical approaches have been proposed to describe acoustics in simplified configurations at low cost [4,5,8,16,32–35]. In particular, this last approach allows the investigation of the underlying mechanisms involved in acoustic phenomena since explicit expressions of acoustic sources or growth rates of modes are obtained.

These low-order methods for thermoacoustics are usually based on a one-dimensional formalism in which acoustic waves are propagated in a network. A paradox arises from the fact that acoustic modeling is usually performed at zero Mach number ($\bar{u}_0 = 0$) while

* Corresponding author at: CERFACS, CFD Team, 42 Av Coriolis, 31057 Toulouse, France.
E-mail addresses: bauerheim@cerfacs.fr, Mich_fdp@hotmail.com (M. Bauerheim).

http://dx.doi.org/10.1016/j.combustflame.2014.06.017

combustion is a process necessarily place at non zero Mach number (otherwise reactants are frozen and are never transported to the reaction zone leading to zero mean heat release $\overline{Q}_0 = 0$, i.e. no temperature or density gradients). A common approach is therefore to consider two "worlds": the first one is the "acoustic world" at zero Mach number and the second one is a "convective world" required by the flame to create the density/temperature gradients at the flame front. Flame Transfer Functions used in Helmholtz solvers are a typical example of how a convective quantity – the time-delay – is incorporated into the "acoustic world" which assumes a zero Mach number. Low-order models are usually prone to this paradox when dealing with acoustic jump conditions required to link fluctuating acoustic quantities at both sides of a thin flame: for a thin flame located at a section change (Fig. 1) in the limit of zero Mach number, typical thermoacoustics studies [11,17,21,30,33,35–40] incorporate a jump condition corresponding to the continuity of the volume flow rate to express velocity perturbation u'_1 and u'_2 on both sides of the flame:

$$u'_1 A_1 = u'_2 A_2 \tag{1}$$

while the intuitive condition would be to write mass conservation:

$$\bar{\rho}_1 u'_1 A_1 = \bar{\rho}_2 u'_2 A_2 \tag{2}$$

which includes the mean density values on both sides of the flame and differs strongly from Eq. (1). Mass conservation is actually used at non-zero Mach numbers by some authors [18,36,41–43], leading to some confusion in the community. The question becomes more complex in network models where Mach number can be zero in certain parts of the combustion chamber modeled as one-dimensional tubes and non null in others (Fig. 1). A crucial question is therefore to prove the consistency between jump conditions at non-null Mach number ($M \neq 0$) and the limit case when the Mach number goes to zero ($M \to 0$). Moreover, the differences between Eqs. (1) and (2) are large because the ratio $\bar{\rho}_1/\bar{\rho}_2$ is of the order of 5–10 in most flames. Using Eq. (1) or (2) leads to very different results in Helmholtz solvers. Therefore, understanding which velocity jump condition must be used is a critical building block in all Helmholtz formulations which clearly requires a careful analysis.

The present paper tries to elucidate this paradox by deriving jump conditions for mass and volume flow rates on a thin flame front at zero and non-zero Mach number. The first starting point is to write the mass conservation at non-null Mach number (Section 2.1). This balance equation is valid but does not degenerate simply to the proper equation at zero Mach number where the volume flow rate is conserved and not the mass flow rate [11]. Another starting point is to write the conservation of total enthalpy at the interface (Section 2.2), which leads to volume flow rate conservation (Eq. (1)) for zero Mach numbers. Showing why these approaches are actually compatible is one goal of the present paper. To achieve this, jump conditions for both mass ($\hat{m} = \bar{\rho}_0 \hat{u} A + \hat{\rho} \bar{u}_0 A$) and volume ($\hat{v} = \hat{u} A$) flow rate perturbations are derived in a case corresponding to two tubes connected by a passive flame and section change (Fig. 1). From the three-dimensional mass balance equation, a quasi-one dimensional mass balance equation is obtained for surface-averaged quantities in Section 2. Then the mass flow rate conservation equation is derived in Section 2.1 for all Mach numbers. This equation couples the unsteady mass flow rate $\hat{m}$ and the entropy fluctuations $\hat{s}$. In addition, a conservation equation for the volume flow rate is also obtained in Section 2.2, which couples the unsteady flow rate $\hat{v}$ and the fluctuating pressure $\hat{p}$. The comparison of the mass and volume flow rate equations in Section 2.3 shows that entropy $\hat{s}$ and pressure gradient $\frac{d\hat{p}}{dx}$ singularities present in these equations change with the Mach number and explains why mass flow rate is conserved at non-null Mach numbers (Section 3) and volume flow rate at zero Mach number (Section 4) demonstrating the consistency between the two formulations.

2. Mass and volume flow rate formulation

The conservation of the fluctuating mass and volume flow rate through the thin flame front of Fig. 1 is described for a configuration with a "steady" flame, i.e. no heat release fluctuations ($\widehat{Q} = 0$) and $\rho_1 > \rho_2$ due to a different temperature in the fresh mixture (subscript 1) and the hot mixture (subscript 2). No distinction between null or non-null Mach number is necessary at this step.

2.1. Mass flow rate ($\hat{m}$)/entropy ($\hat{s}$) coupled equations

The local mass conservation reads:

$$\frac{\partial \rho}{\partial t} = -div(\rho u) \tag{3}$$

where ρ and u are instantaneous three-dimensional quantities.

Since the case studied is quasi-one-dimensional, a spatial averaging over the area A is applied:

$$\overline{F} = \frac{1}{\bar{\rho} A} \int_A \rho F dA \tag{4}$$

where F corresponds to any quantity such as pressure and velocity and $\bar{\rho} = \frac{1}{A} \int_A \rho dA$.

Eqs. (3) and (4) lead to a one-dimensional mass balance equation:

$$A \frac{\partial \bar{\rho}}{\partial t} = -\frac{\partial}{\partial x}(\bar{\rho} \bar{u} A) \tag{5}$$

This equation can be linearized around the mean state:

$$A \frac{\partial \rho'}{\partial t} = -\frac{\partial}{\partial x}(\rho' \bar{u}_0 A + \bar{\rho}_0 u' A) \tag{6}$$

where any one-dimensional quantity $\overline{F}$ is decomposed as $\overline{F} = \overline{F}_0 + F'$ where $\overline{F}_0$ is the mean quantity and F' is the fluctuating part. The second-order term $\rho' u' A$ has been neglected.

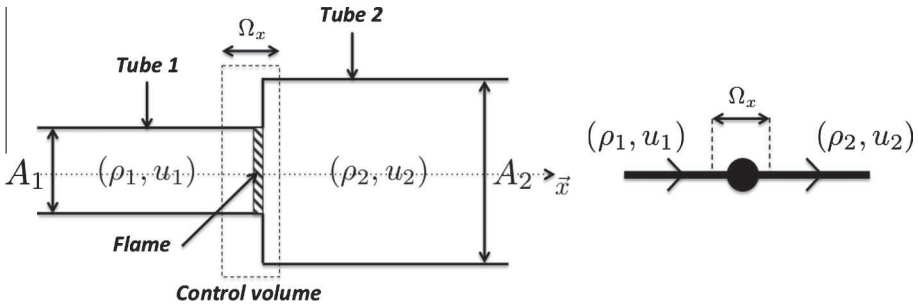

Fig. 1. Configuration (left) with the corresponding one-dimensional model (right) and the control volume (---): two tubes connected by a flame and an abrupt change of section from A_1 to A_2.

Using the Fourier transform of the fluctuation parts $F'(x,t) = \hat{F}(x)e^{-j\omega t}$ and integrating Eq. (6) over the control volume of width Ω_x (Fig. 1) yields:

$$-j\omega\int_{\Omega_x} A\hat{\rho}dx = -\int_{\Omega_x}\frac{d}{dx}(\hat{\rho}\bar{u}_0A+\bar{\rho}_0\hat{u}A)dx = -\int_{\partial\Omega_x}\hat{\rho}\bar{u}_0Adx - \int_{\partial\Omega_x}\bar{\rho}_0\hat{u}Adx \tag{7}$$

where $\partial\Omega_x$ is the boundary of the integration line Ω_x.

The left-hand-side term of the above equation can be recast using the entropy and pressure fluctuations variable knowing that:

$$\hat{\rho} = \frac{\hat{p}}{\bar{c}_0^2} - \frac{\bar{\rho}_0}{C_p}\hat{s} \tag{8}$$

where $\bar{c}_0 = \sqrt{\gamma r\overline{T}_0} = \sqrt{\gamma\bar{p}_0/\bar{\rho}_0}$ is the mean sound speed and C_p is the heat capacity at constant pressure.

The left-hand term of Eq. (7) then becomes:

$$-j\omega\int_{\Omega_x} A\hat{\rho}dx = -j\omega\int_{\Omega_x}\frac{A\hat{p}}{\bar{c}_0^2}dx + j\omega\int_{\Omega_x}\frac{A\bar{\rho}_0\hat{s}}{C_p}dx \tag{9}$$

Finally, injecting Eq. (9) into Eq. (7) and taking the limit $\Omega_x \to 0$ leads to:

$$\lim_{\Omega_x\to 0} -j\omega\int_{\Omega_x}\frac{A\bar{\rho}_0\hat{s}}{C_p}dx = \underbrace{[\hat{\rho}\bar{u}_0A]_1^2 + [\bar{\rho}_0\hat{u}A]_1^2}_{\text{Fluctuating mass flux } \hat{m}} = [\hat{m}]_1^2 \tag{10}$$

where $[F]_1^2 = F_2 - F_1$ stands for the jump of the quantity F at the flame location $x = x_f$ between 1 and 2 (Fig. 1). Note that the acoustic pressure being bounded,[1] the first term of the right-hand side of Eq. (9) goes to zero with Ω_x. This equation couples the jump of fluctuating mass flow rate $[\hat{m}]_1^2$ and the fluctuating entropy $\hat{s}$ at the flame front as already suggested by Dowling [36]. It shows that the unsteady mass flow rate $\hat{m}$ is not necessarily conserved through the flame: it depends on the entropy $\hat{s}$ (or density) variation through the flame front, showing that an additional equation for entropy variation is needed (Section 3) to obtain the final jump condition.

2.2. Volume flow rate ($\hat{v}$)/pressure ($\hat{p}$) formulation

A useful alternative to the mass flow rate conservation equation (Eq. (10)), which involves the fluctuating mass flux $\hat{m} = \hat{\rho}\bar{u}_0A + \bar{\rho}_0\hat{u}A$, is to write an equation for the fluctuating volume flow rate $\hat{v} = \hat{u}A$. This volume jump condition is obtained from the linearized mass balance equation (Eq. (6)) and therefore is equivalent to the previous mass jump condition. However, different source terms appear in both formulations and allow to understand which quantity is conserved depending on the Mach number.

Differentiating over time Eq. (8) gives for complex amplitudes:

$$-j\omega\hat{\rho} = -j\omega\frac{\hat{p}}{\bar{c}_0^2} + j\omega\frac{\bar{\rho}_0}{C_p}\hat{s} \tag{11}$$

The entropy fluctuations are obtained from the convection of entropy, which reads in linearized form:

$$-j\omega\hat{s} + \bar{u}_0\frac{d\hat{s}}{dx} + \hat{u}\frac{d\bar{s}_0}{dx} = 0 \tag{12}$$

where there is no unsteady entropy source term because a steady flame is considered here.[2]

Injecting the expression of $j\omega\hat{s}$ from Eq. (12) into Eq. (11) leads to:

$$-j\omega\hat{\rho} = -j\omega\frac{\hat{p}}{\bar{c}_0^2} + \frac{\bar{\rho}_0\bar{u}_0}{C_p}\frac{d\hat{s}}{dx} + \frac{\bar{\rho}_0\hat{u}}{C_p}\frac{d\bar{s}_0}{dx} \tag{13}$$

Multiplying Eq. (13) by the area A and injecting the mass balance equation $-j\omega\hat{\rho}A = -\frac{d}{dx}(\bar{\rho}_0\hat{u}A + \hat{\rho}\bar{u}_0A)$ (see Eq. (6)) yields:

$$-\frac{d}{dx}(\bar{\rho}_0\hat{u}A + \hat{\rho}\bar{u}_0A) = -j\frac{\omega A}{\bar{c}_0^2}\hat{p} + \frac{\bar{\rho}_0\bar{u}_0A}{C_p}\frac{d\hat{s}}{dx} + \frac{\bar{\rho}_0\hat{u}A}{C_p}\frac{d\bar{s}_0}{dx} \tag{14}$$

The mean entropy gradient $\frac{d\bar{s}_0}{dx}$ is related to the mean pressure and density gradients by differentiating $\bar{s}_0 = -C_p\ln(\bar{\rho}_0/\rho_0) + C_v\ln(\bar{p}_0/p_0)$ where ρ_0 and p_0 are constant reference quantities. Assuming constant heat capacities:

$$\frac{d\bar{s}_0}{dx} = -\frac{C_p}{\bar{\rho}_0}\frac{d\bar{\rho}_0}{dx} + \frac{C_p}{\bar{c}_0^2\bar{\rho}_0}\frac{d\bar{p}_0}{dx} \tag{15}$$

Since the mean entropy gradient $\frac{d\bar{s}_0}{dx}$ is known (Eq. (15)), extracting the volume flow rate $\hat{v} = \hat{u}A$ using $\frac{d}{dx}(\bar{\rho}_0\hat{u}A) = \bar{\rho}_0\frac{d\hat{v}}{dx} + \hat{v}\frac{d\bar{\rho}_0}{dx}$ gives one local equation for the volume flow rate $\hat{v}$:

$$\left(\frac{1}{\bar{c}_0^2}\frac{d\bar{p}_0}{dx} + \bar{\rho}_0\frac{d}{dx}\right)\hat{v} = j\frac{\omega A}{\bar{c}_0^2}\hat{p} - \frac{\bar{\rho}_0\bar{u}_0A}{C_p}\frac{d\hat{s}}{dx} - \frac{d}{dx}(\hat{\rho}\bar{u}_0A) \tag{16}$$

where $\bar{\rho}_0\bar{u}_0A$ is the mean mass flow rate so that this quantity is independent of the axial coordinate x.

The above equation can be simplified combining the two RHS fluxes and using the equation defining the entropy in Eq. (8):

$$\frac{\bar{\rho}_0\bar{u}_0A}{C_p}\frac{d\hat{s}}{dx} + \frac{d}{dx}(\hat{\rho}\bar{u}_0A) = \frac{d}{dx}\left(\frac{\bar{\rho}_0\bar{u}_0A}{C_p}\hat{s} + \hat{\rho}\bar{u}_0A\right) = \frac{d}{dx}\left(\bar{\rho}_0\bar{u}_0A\frac{\hat{p}}{\gamma\bar{p}_0}\right) = \bar{\rho}_0\bar{u}_0A\frac{d}{dx}\left(\frac{\hat{p}}{\gamma\bar{p}_0}\right) \tag{17}$$

Therefore, the expression of the local equation of the volume flow rate conservation (Eq. (16)) reads:

$$-j\omega A\frac{\hat{p}}{\gamma\bar{p}_0} + \bar{v}_0\frac{d}{dx}\left(\frac{\hat{p}}{\gamma\bar{p}_0}\right) + \frac{\hat{v}}{\gamma\bar{p}_0}\frac{d\bar{p}_0}{dx} = -\frac{d\hat{v}}{dx} \tag{18}$$

where $\bar{v}_0 = \bar{u}_0A$ is the mean volume flow rate.

Finally, integrating over the line Ω_x and taking the limit $\Omega_x \to 0$ leads to:

$$\lim_{\Omega_x\to 0}\int_{\Omega_x}\bar{v}_0\frac{d}{dx}\left(\frac{\hat{p}}{\gamma\bar{p}_0}\right)dx + \lim_{\Omega_x\to 0}\int_{\Omega_x}\frac{\hat{v}}{\gamma\bar{p}_0}\frac{d\bar{p}_0}{dx}dx = -[\hat{u}A]_1^2 = -[\hat{v}]_1^2 \tag{19}$$

Note that the acoustic pressure being bounded, the first LHS term of Eq. (18) goes to zero in Eq. (19). Compared to the mass flow rate conservation equation, which couples the mass flow rate $\hat{m}$ and the entropy $\hat{s}$, now, the volume flow rate $\hat{v}$ conservation is linked to the mean $\frac{d\bar{p}_0}{dx}$ and fluctuating $\frac{d\hat{p}}{dx}$ pressure gradients as summarized in Table 1.

Table 1
Summary of the mass and volume flow rate conservation equations obtained in Eqs. (10) and (19).

Jump	Expression
Mass flow rate ($\hat{m} = \hat{\rho}\bar{u}_0A + \bar{\rho}_0\hat{u}A$)	$\lim_{\Omega_x\to 0} -j\omega\int_{\Omega_x}\frac{A\bar{\rho}_0\hat{s}}{C_p}dx = [\hat{\rho}\bar{u}_0A + \bar{\rho}_0\hat{u}A]_1^2$
Volume flow rate ($\hat{v} = \hat{u}A$)	$-\lim_{\Omega_x\to 0}\int_{\Omega_x}\bar{v}_0\frac{d}{dx}\left(\frac{\hat{p}}{\gamma\bar{p}_0}\right)dx$
	$-\lim_{\Omega_x\to 0}\int_{\Omega_x}\frac{\hat{v}}{\gamma\bar{p}_0}\frac{d\bar{p}_0}{dx}dx = [\hat{u}A]_1^2$

[1] A quantity F is bounded if there is a finite positive number M_F where $\|F\| \leqslant M_F$. It implies that $\|\int_{\Omega_x}F(x)dx\| \leqslant \int_{\Omega_x}\|F(x)\|dx \leqslant \int_{\Omega_x}M_Fdx \leqslant M_F\|\Omega_x\|$ goes to zero when $\Omega_x \to 0$. Note that a bounded quantity F does not necessarily imply that F is continuous. For instance, the fluctuating pressure amplitude $\hat{p}$ at non-null Mach number is discontinuous but is however bounded.

[2] Results with an unsteady flame can be obtained in the same manner by adding a source term $\hat{q}_s$ linked to the unsteady heat release on the right-hand side of this equation. This will not change the conclusions of the paper and this term is omitted here for simplicity.

Table 2
LHS source terms in mass ($\dot{m} = \bar{\rho}_0 \hat{u} A + \hat{\rho} \bar{u}_0 A$, top) and volume flow rate ($\dot{v} = \hat{u} A$, bottom) conservation equations (Eqs. (10) and (19)) with the analytical expressions of the singularities depending on the Mach number. δ-singularities act like additional source terms and are colored in gray.

Eq.	Source term	$M = 0$	$M \neq 0$
$\hat{m}$	$-j\omega \int_{\Omega_x} \frac{A\bar{\rho}_0 \hat{s}}{C_p} dx$	$\hat{s} = -j\frac{K_s}{\omega}\hat{u}\delta(x - x_f)$	$\hat{s} = -k e^{j\omega\tau_c(x)} \mathcal{H}(x - x_f)$
$\hat{v}$	$\int_{\Omega_x} \bar{v}_0 \frac{d}{dx}\left(\frac{\hat{p}}{\gamma \bar{p}_0}\right) dx$	$\frac{d}{dx}\left(\frac{\hat{p}}{\gamma \bar{p}_0}\right) = \frac{j\omega}{\bar{c}_0^2}(\hat{u}_2 - \hat{u}_1)\mathcal{H}(x - x_f)$	$\frac{d}{dx}\left(\frac{\hat{p}}{\gamma \bar{p}_0}\right) = \frac{1}{\gamma}\left(\frac{\hat{p}_2}{\bar{p}_{0,2}} - \frac{\hat{p}_1}{\bar{p}_{0,1}}\right)\delta(x - x_f)$
	$\int_{\Omega_x} \frac{\dot{v}}{\gamma \bar{p}_0} \frac{d\bar{p}_0}{dx} dx$	$\frac{1}{\gamma \bar{p}_0} \frac{d\bar{p}_0}{dx} = 0$	$\frac{1}{\gamma \bar{p}_0} \frac{d\bar{p}_0}{dx} = \frac{1}{\gamma} \ln\left(\frac{\bar{p}_{0,2}}{\bar{p}_{0,1}}\right)\delta(x - x_f)$

2.3. Singularities and source terms of conservation equations

Eqs. (10) and (19) are valid for all Mach numbers. They correspond to balance equations coupling the acoustic ($\hat{p}$ or $\hat{u}$) and the entropy ($\hat{s}$ or $\hat{\rho}$) disturbances as suggested by Dowling [36]. They involve integrated LHS source terms, which are not necessarily null and control the jump in mass and volume flow rates.

The LHS terms of Eqs. (10) and (19) depend on integral terms written as $\lim_{\Omega_x \to 0} \int_{\Omega_x} F(x)dx$. Such terms are zero if the quantity $F(x)$ is bounded (but can be discontinuous) on Ω_x: for instance the Heaviside function $F(x) = \mathcal{H}(x)$ would lead to a null source term while a dirac function $F(x) = \delta(x)$ would generate a source term because $\lim_{\Omega_x \to 0} \int_{\Omega_x} \delta(x)dx = 1$.

δ-singularities are present in the two conservation equations Eqs. (10) and (19). Table 2 reveals the reason of the apparent paradox discussed in this paper: different jump conditions are obtained at zero and non-zero Mach numbers because the mathematical nature of these singularities[3] changes with the Mach number. For instance, the presence of an entropy source term in the mass conservation equation shows that an entropy singularity is induced in the flow, which can be smoothed and convected downstream only in the presence of a mean flow. A quiescent flow however prevents this singularity to leave the domain and creates an additional source term to the mass conservation equation as already shown by Nicoud and Wieczorek [44] using Euler simulations of flames at several Mach numbers (Fig. 2).

Consequently the resolutions at non-null ($M > 0$, Section 3) and null ($M = 0$, Section 4) Mach number have to be performed separately. It will be shown that the mass flow rate conservation at non-null Mach number and the volume flow rate conservation at zero Mach number are consistent and directly linked to the entropy $\hat{s}$ and pressure gradients $\frac{d\bar{p}_0}{dx}$ and $\frac{d\bar{p}}{dx}$ behaviors as shown in Table 2 and Fig. 2.

3. Jump condition at non-null Mach number ($M > 0$)

At non-null Mach number, the mean pressure $\bar{p}_0$ and fluctuating pressure $\hat{p}$ are discontinuous (Fig. 2) because of the mean velocity as shown by the integrated mean and unsteady momentum balance equations (Eqs. (20) and (21)) [44]:

$$[\bar{p}_0 + \bar{\rho}_0 \bar{u}_0 \bar{u}_0]_1^2 = 0 \text{ (Mean momentum)} \tag{20}$$

$$[\hat{p} + 2\bar{\rho}_0 \bar{u}_0 \hat{u} + \hat{\rho} \bar{u}_0 \bar{u}_0]_1^2 = 0 \text{ (Linearized unsteady momentum)} \tag{21}$$

Consequently, according to Table 2, additional source terms are present due to the singular pressure gradients in the volume flow rate equation (Eq. (19)) and the volume flow rate $\hat{v} = \hat{u}A$ is not conserved though the interface.

Thus this section will focus on the mass flow rate Eq. (10), which couples the mass flow rate $\hat{m}$ and the entropy $\hat{s}$: the mass flow rate conservation equation (Eq. (10)) and the entropy convection equation (Eq. (12)) have to be solved together as indicated by Dowling [36]. Equation (12) is required to fix the LHS entropy term $\hat{s}$ in Eq. (10). This equation for entropy is a first order differential equation with a source term due to acoustics $\hat{u}$. Its solution is $\hat{s}(x) = \hat{s}_H(x) + \hat{s}_P(x)$ where $\hat{s}_H$ is the solution of Eq. (12) without source term (called the homogeneous equation) and $\hat{s}_P$ is one particular solution of Eq. (12).

3.1. The homogeneous solution $\hat{s}_H$

$\hat{s}_H$ is the solution of the homogeneous equation:

$$-j\omega\hat{s} + \bar{u}_0 \frac{d\hat{s}}{dx} = 0 \tag{22}$$

where $\bar{u}_0$ is a known non-null function of the axial coordinate x:

$$\begin{cases} \bar{u}_0(x) = \bar{u}_{0,1} \text{ if } x \leqslant x_f \\ \bar{u}_0(x) = \bar{u}_{0,2} = \beta \bar{u}_{0,1} \text{ if } x > x_f \end{cases} \tag{23}$$

where $\beta = \frac{\bar{\rho}_{0,1} A_1}{\bar{\rho}_{0,2} A_2}$ is obtained from the mean mass conservation $[\bar{\rho}_0 \bar{u}_0 A]_1^2 = 0$.

The solution $\hat{s}_H$ of the homogeneous Eq. (22) reads:

$$\hat{s}_H(x) = \alpha_s e^{j\omega \int \frac{dx}{\bar{u}_0(x)}} \tag{24}$$

where α_s is a constant to be determined from boundary conditions.

Eq. (24) is valid only at non-null Mach number since it involves the characteristic convection time $\tau_c(x) = \int \frac{dx}{\bar{u}(x)}$, which explains the special behavior of the zero Mach number case (where $\tau_c \to \infty$, Section 4). At non-null Mach number, the characteristic convection time can be expressed explicitly using Eq. (23) and noting that $1/\bar{u}_0(x)$ is also constant by parts ($1/\bar{u}_{0,1}$ for $x < x_f$ and $1/\bar{u}_{0,2}$ for $x > x_f$):

[3] The entropy singularity is detailed in Sections 3 and 4. Pressure gradient singularities are not detailed but obtained here assuming a pressure constant by parts or using for non null Mach number cases $j\omega\hat{u} = \frac{1}{\bar{\rho}_0}\frac{d\hat{p}}{dx}$.

$$\tau_c(x) = \int \frac{dx}{\bar{u}(x)} = \begin{cases} x/\bar{u}_{0,1} \text{ if } x \leqslant x_f \\ \frac{1}{\bar{u}_{0,1}}[x_f + (x - x_f)/\beta] \text{ if } x > x_f \end{cases} \quad (25)$$

Finally, the entropy fluctuation $\hat{s}_H(x,t)$ is:

$$\hat{s}_H(x) = \alpha_s e^{j\omega\tau_c(x)} \quad (26)$$

3.2. One particular solution $\hat{s}_P$

To obtain one particular solution of Eq. (12), the method of variation of constants for inhomogeneous linear ordinary differential equations is applied: the solution $\hat{s}_P$ is sought as:

$$\hat{s}_P(x) = \gamma_s(x) e^{j\omega\tau_c(x)} \quad (27)$$

For the particular solution, the source term in Eq. (12) is retained. This term involves the mean entropy gradient, which is due to mean density and pressure gradients (Eq. (15)) at the flame front $x = x_f$. Because of the abrupt jump of mean density and pressure through the flame front, the mean entropy gradient is singular:

$$\frac{d\bar{s}_0}{dx} = K_s \delta(x - x_f) \quad (28)$$

Using Eqs. (12) and (27) and the expression of the mean density gradient (Eq. (28)) leads to the following equation for $\gamma_s(x)$:

$$\frac{d\gamma_s(x)}{dx} = -K_s \frac{\hat{u}(x)}{\bar{u}_0(x)} e^{-j\omega\tau_c(x)} \delta(x - x_f) \quad (29)$$

whose solutions are:

$$\gamma_s(x) = -K_s \left[\frac{\hat{u}}{\bar{u}_0}\right]^*_{x=x_f} e^{-j\omega\tau_c(x_f)} H(x - x_f) \quad (30)$$

where $[f]^*_{x=x_f}$ is the value of the regularized function f at $x = x_f$, i.e. $\frac{1}{2}(f(x = x_f^+) + f(x = x_f^-))$.

The final expression for the particular solution $\hat{s}_P(x)$ is:

$$\hat{s}_P(x) = -K_s \left[\frac{\hat{u}}{\bar{u}_0}\right]^*_{x=x_f} e^{j\omega[\tau_c(x) - \tau_c(x_f)]} H(x - x_f) \quad (31)$$

3.3. Solution of the convection equation for the entropy fluctuations and mass conservation at non-null Mach number ($M > 0$)

The solution of the full convective Eq. (12) is thus the sum of the homogeneous and particular solutions (Eqs. (26) and (31)):

$$\hat{s}(x) = \hat{s}_H(x) + \hat{s}_P(x) = \alpha_s e^{j\omega\tau_c(x)} - K_s \left[\frac{\hat{u}}{\bar{u}_0}\right]^*_{x=x_f} e^{j\omega[\tau_c(x) - \tau_c(x_f)]} H(x - x_f) \quad (32)$$

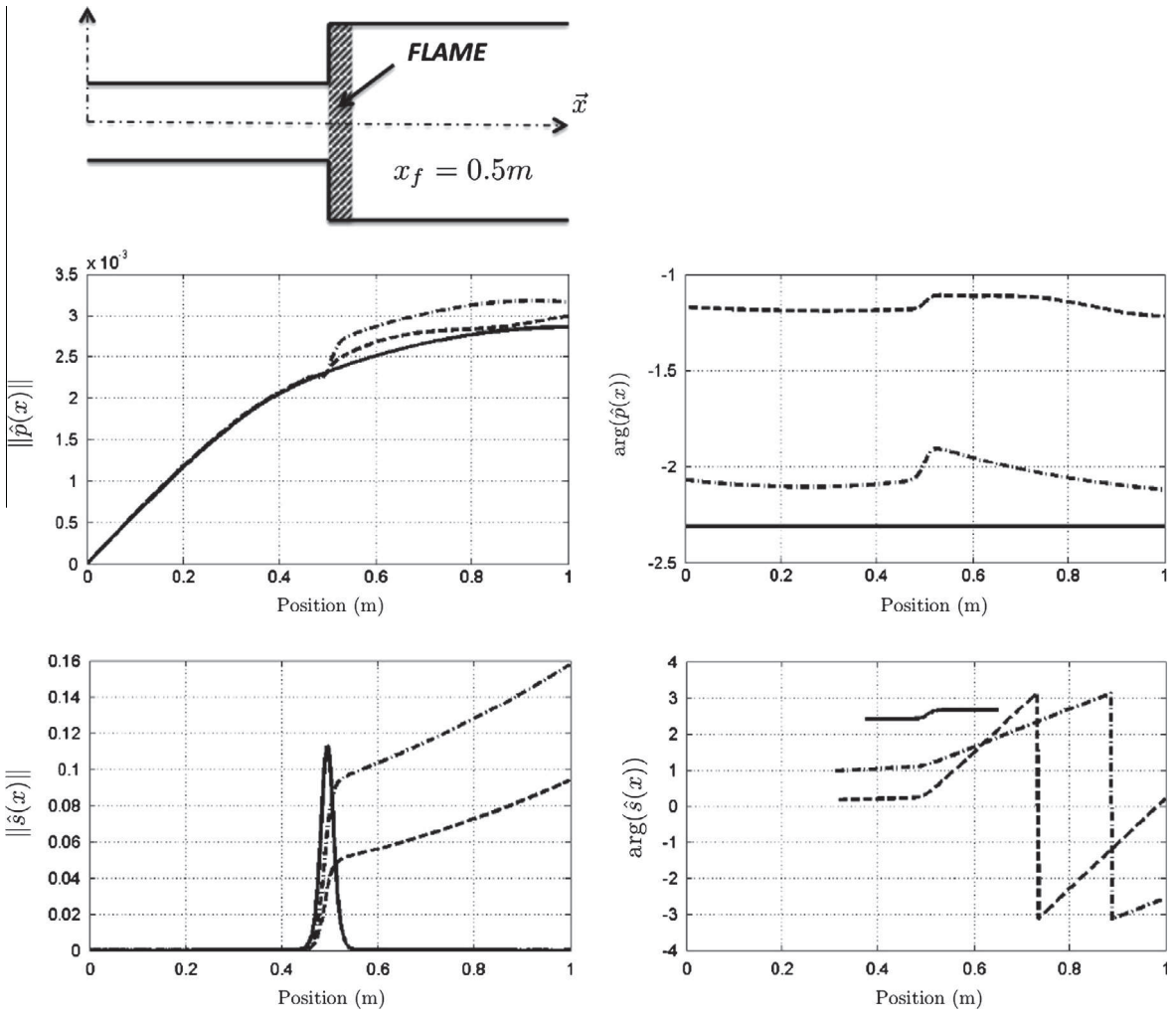

Fig. 2. The Normalized pressure (top) and entropy (bottom) modulus (left) and phase (right) obtained by Nicoud and Wieczorek [44] for several Mach numbers in a straight tube of constant cross section: —: $M = 0$ (thickened entropy spot at $x = x_f = 0.5$ m and continuous pressure), - - -: $M = 0.05$ (entropy convected downstream and discontinuous pressure) and -·-·-: $M = 0.11$ (entropy convected downstream and discontinuous pressure).

Assuming zero entropy fluctuations coming from the upstream end of the configuration ($x = 0$) leads to $\alpha_s = 0$ and finally:

$$\hat{s}(x) = -K_s \left[\frac{\hat{u}}{\bar{u}_0}\right]_{x=x_f}^{*} e^{j\omega\left[\tau_c(x)-\tau_c(x_f)\right]} H(x - x_f) \tag{33}$$

In other words, this result shows (Appendix A) that a flame excited by acoustic waves $\hat{u} \neq 0$ at non-null Mach number ($\bar{u}_0 > 0$) generates entropy fluctuations, which are convected downstream.

Eq. (33) shows that at non-null Mach number ($M > 0$) the entropy fluctuations are bounded although discontinuous at $x = x_f$. It follows that the LHS term in Eq. (10) goes to zero when the volume $\Omega_x S$ tends to zero:

$$\lim_{\Omega_x \to 0} -j\omega \int_{\Omega_x} \frac{A\bar{\rho}_0 \hat{s}}{C_p} dx = 0 \tag{34}$$

which leads directly to the mass conservation through the flame at non-null Mach number:

$$[\hat{\rho}\bar{u}_0 A]_1^2 + [\bar{\rho}_0 \hat{u} A]_1^2 = [\hat{m}]_1^2 = 0 \tag{35}$$

4. Analysis of the mass and volume conservation at zero Mach number ($M = 0$)

A well known paradox arises from Eq. (35) when considering an infinitely thin flame at zero Mach number ($M = 0$). Indeed, using Eq. (35) and enforcing $\bar{u}_0 = 0$ does not yield the proper equation of volume flow rate conservation [36]. The derivation of Eq. (32) in Section 3 requires divisions by $\bar{u}_0$ and therefore cannot be extended to cases at zero Mach number. For these cases, an alternative solution is to start from the total enthalpy $mH = \rho u A(C_p T + \frac{1}{2}u^2)$ conservation, which reads [44]:

$$\left[\left(C_p \overline{T}_0 + \frac{1}{2}\bar{u}_0^2\right)(\bar{\rho}_0 \hat{u} + \hat{\rho}\bar{u}_0)A + \bar{\rho}_0 \bar{u}_0 A\left(C_p \widehat{T} + \bar{u}_0 \hat{u}\right)\right]_1^2 = \widehat{Q} \tag{36}$$

where $[F]_1^2$ corresponds to the jump of any quantity F: $[F]_1^2 = F_2 - F_1$ and $\widehat{Q} = 0$ since here a steady flame is considered for the sake of simplicity (this does not change the result of this demonstration).

When the mean velocity goes to zero (i.e. $\bar{u}_0 = 0$), this relation goes naturally to the volume flow rate conservation:

$$\left[C_p \overline{T}_0 \bar{\rho}_0 \hat{u} A\right]_1^2 = 0 \iff [\hat{u}A]_1^2 = 0 \tag{37}$$

since the flame is an isobaric element at zero Mach number so that $\bar{p}_0 = R\bar{\rho}_0 \overline{T}_0$ is conserved.

This result can also be obtained using the volume flow rate conservation equation (Eq. (19)), which couples the unsteady volume $\hat{v}$ and pressure $\hat{p}$. At null Mach number, the mean and fluctuating pressure are continuous:

$$[\bar{p}_0]_1^2 = 0 \quad \text{and} \quad [\hat{p}]_1^2 = 0 \tag{38}$$

Thus, the two source terms present in the volume flow rate equation (Eq. (19)) are null (Fig. 2): the volume flow rate conservation at zero Mach number results from the pressure continuity at the interface. It also appears from the volume flow rate equation (Eq. (19)) or the total entropy equation (Eq. (36)) that formulations, which already incorporate the entropy equation will degenerate naturally toward the volume flow rate conservation at zero Mach number.

The problem is therefore not to prove the volume flow rate conservation (Eq. (37)) at zero Mach number but to demonstrate its consistency with the mass flow rate conservation (Eq. (35)) at non-null Mach number and to highlight its intrinsic links with singularities of the entropy fluctuations as depicted in the previous section.

Considering the mass balance equation at zero Mach number, Eq. (10) still holds but Eq. (35) does not because the entropy fluctuations $\hat{s}$ in Eq. (10) are not bounded anymore. At zero Mach number, the mathematical nature of the entropy equation (Eq. (12)) changes and now reads:

$$-j\omega\hat{s} + \hat{u}\frac{d\bar{s}_0}{dx} = 0 \tag{39}$$

where $\frac{d\bar{s}_0}{dx} = -\frac{C_p}{\bar{\rho}_0}\frac{d\bar{\rho}_0}{dx} = -C_p \frac{d\ln(\bar{\rho}_0)}{dx} = -C_p \ln\left(\frac{\bar{\rho}_{0,2}}{\bar{\rho}_{0,1}}\right)\delta(x - x_f)$ for an isobaric transformation with a mean density constant by parts: $\bar{\rho}_{0,1}$ for $x < x_f$ and $\bar{\rho}_{0,2}$ for $x > x_f$. The solution of Eq. (38) is:

$$\hat{s} = j\frac{C_p \hat{u}}{\omega\bar{\rho}_0}\frac{d\bar{\rho}_0}{dx} = j\frac{C_p}{\omega}\ln\left(\frac{\bar{\rho}_{0,2}}{\bar{\rho}_{0,1}}\right)\hat{u}\delta(x - x_f) \tag{40}$$

Eq. (40) proves that, at zero Mach number, the entropy fluctuation $\hat{s}$ is a δ-singularity located at the flame position $x = x_f$, also observed in [44] (— in Fig. 2): the left-hand term of Eq. (10) does not go to zero and the mass balance equation does not degenerate toward the mass conservation at the interface: $[\hat{m}]_1^2 \neq 0$.

To demonstrate the consistency between the two formulations ($\hat{m} - \hat{s}$ and $\hat{v} - \hat{p}$), the source term of the mass flow balance equation can be integrated using Eq. (40):

$$\begin{aligned}\lim_{\Omega_x \to 0} -j\omega \int_{\Omega_x} \frac{A\bar{\rho}_0 \hat{s}}{C_p} dx &= \lim_{\Omega_x \to 0} \int_{\Omega_x} \hat{u}A\frac{d\bar{\rho}_0}{dx} dx \\ &= [\bar{\rho}_0 \hat{u}A]_1^2 - \lim_{\Omega_x \to 0} \int_{\Omega_x} \bar{\rho}_0 \frac{d\hat{u}A}{dx} dx\end{aligned} \tag{41}$$

Combining the mass flow rate conservation (Eq. (10)) and the integration of the source term (Eq. (41)) shows that the entropy singularity compensates one part of the mass flow rate (the one independent of the Mach number: $\bar{\rho}_0 \hat{u}A$). Since at zero Mach number the second part of the mass flux $\hat{\rho}\bar{u}_0 A$ is null it yields:

$$\cancel{[\bar{\rho}_0 \hat{u}A]_1^2} - \lim_{\Omega_x \to 0} \int_{\Omega_x} \bar{\rho}_0 \frac{d\hat{u}A}{dx} dx = \cancel{[\bar{\rho}_0 \hat{u}A]_1^2} + \underbrace{[\hat{\rho}\bar{u}_0 A]_1^2}_{=0 \text{ at } M=0} \tag{42}$$

Consequently $\lim_{\Omega_x \to 0} \int_{\Omega_x} \bar{\rho}_0 \frac{d\hat{u}A}{dx} dx = 0$. In other words $\frac{d\hat{u}A}{dx}$ is bounded at $x = x_f$, which means that $[\hat{u}A]_1^2 = 0$.[4] This proves that the mass conservation at non-null Mach number and the volume flow rate conservation at zero Mach number are consistent: at zero Mach number, the entropy $\hat{s}$ generated by the flame excited by the acoustics $\hat{u}$ is stuck at the flame location x_f due to the frozen flow. The singularity of the fluctuating entropy cannot be neglected and is related to the density gradient $\nabla\bar{\rho}_0$ (and the fluctuating heat release $\hat{q}_s$ for an unsteady flame), which leads to the volume flow rate conservation (Eq. (42)).

5. Conclusion

The consistency between conservation equations at zero and non-null Mach number has been proved for the mass/volume flow rate conservation the case of two connected tubes separated by a steady flame. The mass conservation equation is derived for all Mach numbers: it involves source terms coupling the acoustic ($\hat{p}$ or $\hat{u}$) and entropy disturbances ($\hat{s}$ or $\hat{\rho}$). In particular, the nature of entropy singularities changes with the Mach number explains why mass conservation of fluctuations is satisfied at non-zero

[4] This result can be proven by contradiction: let's assume that $\hat{u}A$ contains a discontinuity at the interface (i.e. $\hat{u}A \sim \mathcal{H}(x - x_f)$). Consequently, its derivative contains a δ-singularity (i.e. $d\hat{u}A/dx \sim \delta(x - x_f)$), which leads to $\lim_{\Omega_x \to 0} \int_{\Omega_x} \frac{d\hat{u}A}{dx} dx \neq 0$ in contradiction with Eq. (42). Therefore $\hat{u}S$ is continuous at the interface, i.e. $[\hat{u}A]_1^2 = 0$.

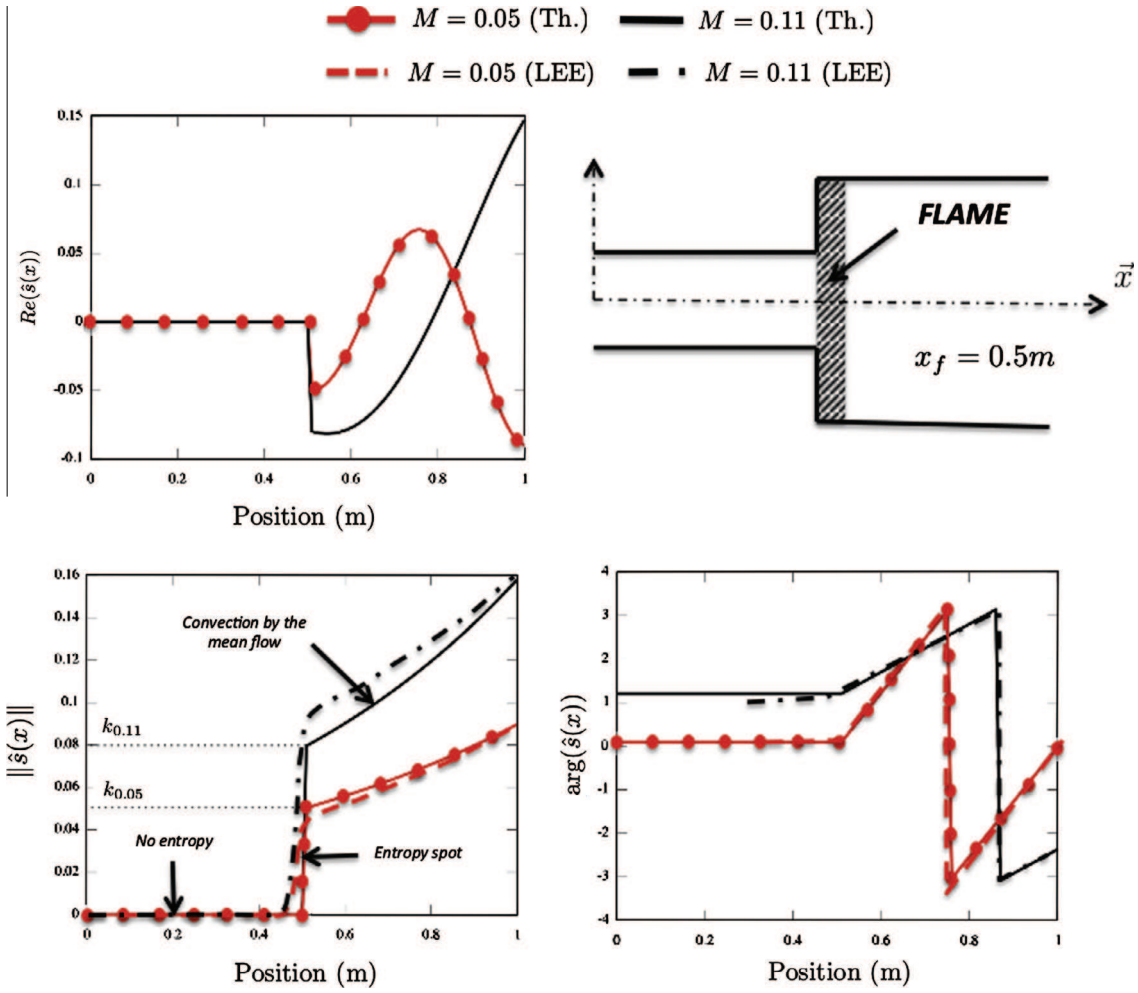

Fig. A.3. Typical shape of the entropy (real part, top left), modulus (bottom, left) and phase (bottom, right) obtained theoretically in Eq. (33) for $M = 0.05$ and $M = 0.11$ cases and corresponding to complex frequencies $f_{0.05} = 139 - 13j$ Hz and $f_{0.11} = 134 - 34j$ Hz. LEE results [44] are superimposed for the entropy modulus $\|\hat{s}\|$ and phase $arg(\hat{s})$.

Mach number while volume flow rate is conserved at zero Mach number.

This conclusion can be discussed using the present analytical results: at non-null Mach number, the entropy generated in the thin flame region is convected by the mean flow. No singularity occurs and leads to the classical mass $\hat{m}$ conservation at the interface.

However, at zero Mach number, the flow is frozen and entropy spots are not convected downstream: they are stuck in the thin flame region producing a singularity related to the mean density gradient, which acts as an additional source term in the mass conservation equation. The proper integration of this source term at zero Mach number leads, not to the mass, but to the volume flow rate conservation as expected. In addition, a balance equation for the volume flow rate $\hat{v}$ has also been derived. This equation couples the volume flow rate $\hat{v}$, the mean pressure $\bar{p}_0$ and the fluctuating pressure $\hat{p}$. It degenerates naturally toward the volume flow rate conservation at the flame interface at zero Mach number because of the pressure continuity.

This theoretical analysis has been systematically compared to LEE simulations of stable flames and a good agreement is found for the entropy fluctuations shape and the conserved quantities.

Appendix A. Comparison between theory and Linearized Euler Equation (LEE) results

The solution of Eq. (33) can be compared to the Linearized Euler Equation (LEE) simulations obtained by Nicoud and Wieczorek [44] displayed in Fig. A.3 for both Mach numbers $M = 0.05$ and $M = 0.11$. The complex frequencies provided in [44] are used to evaluate the formula (33): $f_{0.05} = 139 - 13j$ Hz and $f_{0.11} = 134 - 34j$ Hz. In this case, $\beta = 4$ and $\bar{c}_1 = 347$ m/s. Since normalization of $\hat{s}$ has been performed in [44], the term $k_M = K_s \left[\frac{\hat{u}}{\bar{u}}\right]^*_{x=x_f}$ has been tuned to match the entropy spot at the flame location leading to $k_{0.05} = 0.05$ and $k_{0.11} = 0.08$.

- No entropy is observed upstream of the flame ($x < x_f$) in both LEE simulations and Eq. (33).
- An entropy spot at the flame location ($x = x_f$) is present. In the LEE simulations, the discontinuity is smoothed by the mesh resolution and the thickened flame technique.
- Downstream of the flame ($x > x_f$) the entropy is convected by the mean flow leading to an increasing exponential shape (since stable flames ($Im(\omega) < 0$) are studied in [44]).
- No singularity is present in Eq. (33) and Fig. A.3, which implies that entropy fluctuations are bounded although discontinuous.

References

[1] W.C. Strahle, J. Fluid Mech. 49 (1971) 399–414.
[2] W.C. Strahle, J. Sound Vib. 23 (1972) 113–125.
[3] S. Kotake, J. Sound Vib. 42 (1975) 399–410.
[4] H.S. Tsien, J. Am. Rocket Soc. 22 (1952).
[5] F.E. Marble, S. Candel, J. Sound Vib. 55 (1977) 225–243.
[6] S. Candel, J. Sound Vib. 24 (1972) 87–91.

[7] F. Bake, C. Richter, B. Muhlbauer, N. Kings, I. Rohle, F. Thiele, B. Noll, J. Sound Vib. (2009) 574–598.
[8] M. Leyko, F. Nicoud, T. Poinsot, AIAA J. 47 (2009) 2709–2716.
[9] W. Krebs, P. Flohr, B. Prade, S. Hoffmann, Combust. Sci. Technol. 174 (2002) 99–128.
[10] S. Candel, Proc. Combust. Inst. 29 (2002) 1–28.
[11] T. Poinsot, D. Veynante, Theoretical and Numerical Combustion, third ed., 2011. <www.cerfacs.fr/elearning>.
[12] T. Lieuwen, V. Yang, Combustion Instabilities in Gas Turbine Engines, Operational Experience, Fundamental Mechanisms and Modeling, volume 210, Progress in Astronautics and Aeronautics, AIAA, 2005.
[13] B. Schuermans, V. Bellucci, C. Paschereit, in: International Gas Turbine and Aeroengine Congress & Exposition, ASME Paper, volume 2003-GT-38688.
[14] N. Worth, J. Dawson, Proc. Combust. Inst. 34 (2013) 3127–3134.
[15] N. Worth, J. Dawson, Combust. Flame 160 (2013) 2476–2489.
[16] N. Noiray, M. Bothien, B. Schuermans, Combust. Theory Model. (2011) 585–606.
[17] J. Kopitz, A. Huber, T. Sattelmayer, W. Polifke, in: Int'l Gas Turbine and Aeroengine Congress & Exposition, ASME GT2005-68797, Reno, NV, USA.
[18] S.R. Stow, A.P. Dowling, in: Proceedings of ASME Turbo Expo, GT2003-38168, Atlanta, Georgia, USA.
[19] S. Evesque, W. Polifke, in: International Gas Turbine and Aeroengine Congress & Exposition, ASME Paper, volume GT-2002-30064.
[20] S.R. Stow, A.P. Dowling, in: ASME Paper, 2001-GT-0037, New Orleans, Louisiana.
[21] J. Moeck, M. Paul, C. Paschereit, in: ASME Turbo Expo 2010 GT2010-23577.
[22] J.-F. Bourgouin, D. Durox, J. Moeck, T. Schuller, S. Candel, in: ASME Turbo Expo, GT2013-95010.
[23] K. Kunze, C. Hirsch, T. Sattelmayer, in: ASME Turbo Expo, GT2004-53106.
[24] C. Fureby, Flow, Turb. Combust. 84 (2010) 543–564.
[25] P. Wolf, G. Staffelbach, L. Gicquel, J. Muller, T. Poinsot, Combust. Flame 159 (2012) 3398–3413.
[26] F. Flemming, A. Sadiki, J. Janicka, Proc. Combust. Inst. 31 (2007) 3189–3196.
[27] M. Leyko, F. Nicoud, S. Moreau, T. Poinsot, in: Proc. of the Summer Program, Center for Turbulence Research, NASA AMES, Stanford University, USA, 2008, pp. 343–354.
[28] M. Leyko, F. Nicoud, S. Moreau, T. Poinsot, C.R. Acad. Sci. Méc. 337 (2009) 415–425.
[29] C. Sensiau, F. Nicoud, T. Poinsot, Int. J. Aeroacoust. 8 (2009) 57–68.
[30] G. Campa, S. Camporeale, A. Guaus, J. Favier, M. Bargiacchi, A. Bottaro, E. Cosatto, G. Mori, GT2011-45969.
[31] C. Pankiewitz, T. Sattelmayer, ASME J. Eng. Gas Turb. Power 125 (2003) 677–685.
[32] I. Duran, S. Moreau, J. Fluid Mech. 723 (2013) 190–231.
[33] J. Parmentier, P. Salas, P. Wolf, G. Staffelbach, F. Nicoud, T. Poinsot, Combust. Flame 159 (2012) 2374–2387.
[34] G. Ghirardo, M. Juniper, Proc. Roy. Soc. A 469 (2013).
[35] M. Bauerheim, J. Parmentier, P. Salas, F. Nicoud, T. Poinsot, Combust. Flame 161 (2014) 1374–1389.
[36] A.P. Dowling, J. Sound Vib. 180 (1995) 557–581.
[37] M. Heckl, M. Howe, J. Sound Vib. 305 (2007) 672–688.
[38] A. Kaufmann, F. Nicoud, T. Poinsot, Combust. Flame 131 (2002) 371–385.
[39] G. Gelbert, J. Moeck, C. Paschereit, R. King, Control Eng. Pract. 20 (2012) 770–782.
[40] T. Schuller, D. Durox, P. Palies, S. Candel, Combust. Flame 159 (2012) 1921–1931.
[41] J. Gikadi, T. Sattelmayer, A. Peschiulli, in: Proceeding of ASME Trubo Expo, 2012-69612.
[42] T. Lieuwen, J. Prop. Power 19 (2003) 765–781.
[43] E. Motheau, F. Nicoud, T. Poinsot, Proceeding of ASME Trubo Expo GT2012-68852, 2012.
[44] F. Nicoud, K. Wieczorek, Int. J. Spray Combust. Dynam. 1 (2009) 67–112.